Methane production by mechanochemical processing of MgH2-Li2CO3as sources of H2and CO2at room temperature

Journal of CO_2 Utilization xxx (2019) xxx–xxx

Contents lists available at ScienceDirect

Journal of CO_2 Utilization

journal homepage: www.elsevier.com/locate/jcou

1

Graphical abstract

Methane production by mechanochemical processing of MgH_2-Li_2CO_3 as sources of H_2 and CO_2 at room temperature

María L. Grasso*, Luisa Fernández Albanesi, Sebastiano Garroni, Gabriele Mulas, Fabiana C. Gennari

Journal of CO_2 Utilization xxx (2019) pp. xxx–xxx

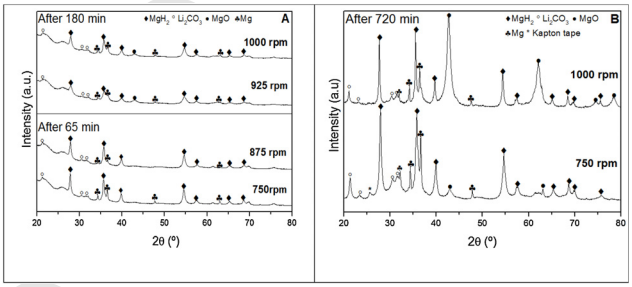

Journal of CO_2 Utilization xxx (2019) xxx–xxx

Contents lists available at ScienceDirect

Journal of CO_2 Utilization

journal homepage: www.elsevier.com/locate/jcou

1

Highlights

Journal of CO_2 Utilization xxx (2019) pp. xxx–xxx

Methane production by mechanochemical processing of MgH_2-Li_2CO_3 as sources of H_2 and CO_2 at room temperature

María L. Grasso*, Luisa Fernández Albanesi, Sebastiano Garroni, Gabriele Mulas, Fabiana C. Gennari

- CH_4/H_2 fuel mixture is obtained by mechanical milling of MgH_2-Li_2CO_3 at room temperature.
- Mechanochemical process occurs without catalyst and with high selectivity to methane.
- Analyses of the gas-product evolution evidences the absence of CO_2 or CO during milling.
- Methane generation is kinetically restricted by the high stability of Li_2CO_3.
- Solid products are reused as CO_2 absorbers for the exhaust gases treatment of power plants.

Journal of CO_2 Utilization xxx (2019) xxx–xxx

Contents lists available at ScienceDirect

Journal of CO_2 Utilization

journal homepage: www.elsevier.com/locate/jcou

Methane production by mechanochemical processing of MgH_2-Li_2CO_3 as sources of H_2 and CO_2 at room temperature

María L. Grasso[a,b,*], Luisa Fernández Albanesi[a,c], Sebastiano Garroni[d], Gabriele Mulas[d], Fabiana C. Gennari[a,c,e]

[a] Consejo Nacional de Investigaciones Científicas y Técnicas (CONICET), R8402AGP, S. C. de, Bariloche, Río Negro, Argentina
[b] Universidad Nacional de Cuyo (UNCuyo), Facultad de Ciencias Exactas y Naturales, M5502JMA, Ciudad de Mendoza, Mendoza, Argentina
[c] Centro Atómico Bariloche (CAB-CNEA), R8402AGP, S.C. de, Bariloche, Río Negro, Argentina
[d] Dipartimento di Chimica e Farmacia and INSTM, Università degli Studi di Sassari, 07100, Sassari, Italy
[e] Universidad Nacional de Cuyo (UNCuyo), Instituto Balseiro, Av. Bustillo 9500, R8402AGP, Bariloche, Río Negro, Argentina

ARTICLE INFO

Article history:
Received 7 May 2020
Received in revised form 29 May 2020
Accepted 6 June 2020
Available online xxx

Keywords:
CO_2 conversion
Alkaline carbonates
Light metal hydrides
Methane
Hydrogen

ABSTRACT

The reutilization of CO_2 to produce valuable chemical fuels is an attractive approach to reduce the greenhouse effect and global warming. In this work, the room temperature production of CH_4/H_2 fuel mixtures via mechanochemical activation of Li_2CO_3-MgH_2 system was explored. The CH_4/H_2 fuel mixtures were obtained by a free-catalyst reaction, with high selectivity and using Li_2CO_3 and MgH_2 as solid portable sources of CO_2 and H_2, respectively. The effect of processing parameters on both the evolution of the solid phases and the production of CH_4/H_2 fuel mixtures was studied using X-ray diffraction, spectroscopic techniques, electron scanning microscopy and gas chromatography. Thermodynamic calculations predict the complete CO_2 reduction to CH_4, with simultaneous formation of MgO and Li_2O. Experimental evidence supports the progressive formation of MgO and the appearance of Li_2O. The presence of H_2 simultaneously with CH_4 in the gas phase was due to kinetic restrictions. Based on experimental results and equilibrium composition calculations, the reaction mechanism was proposed. The kinetic analysis reveals that the rate limiting CH_4 production is the nucleation of MgO/Li_2O in the surroundings of Li_2CO_3, while the H_2 release is controlled by the reaction interface between MgH_2/Mg or MgH_2/MgO.

1. Introduction

Carbon dioxide gas (CO_2) is considered one of the main contributors to global warming and climate change because of its role in the greenhouse effect. Human activities, such as combustion of fossil materials (coal, oil, natural gas), industrial processes, changes in land use and deforestation, are considered to be the main responsible for the growing CO_2 atmospheric concentration, from 280 ppm in the pre-industrial era to 415 ppm in 2019 [1], with an increase of 0.8 °C in global planet temperature. Intergovernmental Panel on Climate Change (IPCC) has estimated that by the end of the century, CO_2 concentration would reach 700 ppm and the average temperature would increase up to 5 °C, with devastating and irreversible climate changes [2]. For these reasons, a current and urgent challenge is to find a sustainable way to reduce CO_2 concentration in the atmosphere. Unfortunately, the continuous increase in energy demand due to a growing population and life-style quality implies more CO_2 atmospheric emissions [3].

Carbon dioxide capture and utilization (CCU) is a very promising strategy to mitigate CO_2 emissions, having at the same time a benefit related to the production of value-added products. Here, CO_2 acts as a carbon source to synthesize products such as alcohols, polymers and synthetic fuels. Also, there are direct applications of the captured CO_2: in carbonated drinks, as dry-ice, in fire extinguishers or in algae farms for photosynthesis [3,4]. Among synthetic fuels to be produced from CO_2, methane is the hydrocarbon with the highest hydrogen to carbon ratio. Its gravimetric heat is greater (55.5 MJ/kg) than butane (49.5 MJ/kg), diesel (44.8 MJ/kg) and methanol (22.7 MJ/kg) [5]. In addition, CH_4 is compatible with our current storage and distribution network. Based on its good properties, methane is considered an attractive and alternative fuel. Interestingly, the addition of H_2 to CH_4 produces a fuel-gas mixture with improved properties for its

* Corresponding author at: Consejo Nacional de Investigaciones Científicas y Técnicas (CONICET), Universidad Nacional de Cuyo (UNCuyo), Facultad de Ciencias Exactas y Naturales, Av. Bustillo 9500, R8402AGP, Bariloche, Río Negro, Argentina.
E-mail address: maria.grasso@cab.cnea.gov.ar (M.L. Grasso).

http://dx.doi.org/10.1016/j.jcou.2020.101209
2212-9820/

use in stationary applications like heaters, boilers and turbines or in mobile applications like internal combustion engines and gas turbines [6,7]. In fact, the wide ignition limits and high flame speed of hydrogen have a positive impact on the combustion, improving the energy density of natural gas on the operation conditions. In addition, mixtures of H_2 with CH_4 allow a substantial reduction of the CO_2 emissions. These hydrogen-enriched mixtures (up to 20 %) can be distributed by the mid-pressure natural gas network or stored under pressure using conventional methane storage technologies without substantial technical modifications [8].

In the search for alternative methods of CO_2 hydrogenation, our working group has recently reported the use of Mg-Fe and Mg-Ni complex hydrides with a dual function: as promoters of the CO_2 conversion and as hydrogen sources [9,10]. CO_2 methanation was promoted by the presence of Fe, Ni and/or Mg-Ni alloys obtained during decomposition of the Mg_2FeH_6 and Mg_2NiH_4 hydrides, while its conversion depended on the nature of the hydride, the experimental conditions and the H_2:CO_2 molar ratio [9]. The global mechanism for both hydrides includes the reversed water-gas shift reaction followed by CO methanation in presence of steam. However, in the case of Mg_2NiH_4, the direct reduction of CO_2 by MgH_2/Mg_2NiH_x hydrides takes an important role in the whole process. Refinement of the Mg_2NiH_4 microstructure to the nanometric scale modifies the CO_2 methanation mechanism [10] and it proceeds by adsorption of C and direct solid gasification toward CH_4 formation.

In this context, the development of simple methods for CO_2 conversion into valuable chemicals or energy carriers under soft conditions (mild pressure and temperature) is a topic of interest in the scientific community. In this respect, the mechanochemical synthesis is considered a manufacturing technology that is simple, efficient, cheap, scalable, low-waste, and solvent-free for the production of chemicals at room temperature [11,12].

Mechanochemical activation of different solids was applied to promote CO_x storage and/or its conversion via different solid-gas reactions [13–17]. Mulas et al. studied the mechanochemical hydrogenation of CO over FeCo and Mg_2Ni-based catalysts [13]. Chemical transformations were promoted by mechanical treatment at the interface of solid-gas systems at mild conditions. The CO_2 conversion to CH_4 obtained *via* FeCo catalysts at room temperature and atmospheric pressure is similar to the corresponding one occurring in thermally activated conditions, which requires high temperature and pressure. In addition, a recent investigation reported the production of CH_4 and light hydrocarbons by milling of the olivine (a magnesium silicate mineral) and water under CO_2 atmosphere [14]. Energetic ball milling promotes the olivine-water activation, releasing H_2 and allowing the hydrogenation of CO_2 by the in situ formation of magnetite-based catalysts [15]. The mechanism of the whole process is complex, and competitive processes such as the precipitation of carbonate phases were also detected as dependent on the CO_2/H_2O ratio. These investigations exhibit the potential of mechanochemical processing to promote gas-solid reactions in the presence of catalysts and under mild conditions.

In this line, two recent investigations reported the mechanochemical conversion of CO_2 to produce CH_4-H_2 mixtures using light metal hydrides (LiH, NaH, MgH_2 and CaH_2) as hydrogen source at room temperature and without any catalyst [16,17]. Dong et al. were the first to produce CO_x-free mixtures of CH_4-H_2 through a solid-gas mechanochemical reaction. The yield of CH_4 was dependent on the nature of the light metal hydride, rate and duration of ball milling, and CO_2 pressure. The selectivity also depends on these parameters, detecting CO formation at high CO_2:H_2 ratios. Experimental results indicated that the mechanism of CO_2 reduction using MgH_2 (or LiH) involves the production of amorphous carbon followed by a hydrogenation step:

$$2MgH_2(s) + CO_2(g) \rightarrow 2\_MgO(s) + C(s) + 2H_2(g) \quad (1)$$

$$C(s) + \ 2H_2(g) \rightarrow CH_4(g) \quad (2)$$

The reaction between carbon and H_2 produced *in situ* during mechanochemical processing is responsible for the CH_4 formation.

Using a similar strategy, Pu et al. investigated the effect of different H_2:CO_2 ratios on the conversion efficiency of CO_2 to CH_4 by mechanochemical reduction with light metal hydrides. According to the X-ray diffraction (XRD), Fourier transform infrared spectroscopy (FTIR) and X-ray photoelectron spectroscopy (XPS) data, the following reaction mechanism was proposed for H_2:CO_2 molar ratio lower than 2:1:

$$4\_MgH_2(s) + 2CO_2(g) \rightarrow 4\_MgO(s) + C(s) + 2\_H_2(g) + \ CH_4(g) \quad (3)$$

As the concentration of CO_2 was increased, CO formation was observed. For H_2:CO_2 ratio of 7:5, the solid products formed were MgO, $MgCO_3$ and C, and the global reaction can be described by:

$$5\_MgH_2(s) + 3CO_2(g) \rightarrow 5\_MgO(s) + C(s) + 3\_H_2(g) + \ CH_4(g) + \ CO(g) \quad (4)$$

$$MgO(s) + CO_2(g) \ \rightarrow MgCO_3(s) \quad (5)$$

These investigations demonstrated that the mechanism of CO_2 reduction by light metal hydrides depends on several factors. In general, LiH and MgH_2 hydrides, contrary to NaH, favor the reduction of CO_2 to CH_4.

Recently, Dong et al. studied the interaction between metal hydrides and alkaline carbonates as sources of H_2 and CO_2, respectively [18]. This study consisted in following the reactivity of MH-M_2CO_3 systems (where M = Mg or Ca) during mechanical milling at room temperature under catalyst-free conditions. The authors reported a highly selective method to CO_2 conversion and to synthesize CO_x free H_2/CH_4 blends. Different parameters such as prolonged milling times of 48 h, high ball milling rates (450−550 rpm), and high H_2:CO_2 ratios promote the formation of CH_4 as the only hydrocarbon product. The analysis of the gas and solid products show that the methanation reaction occurs between the H_2 released from the hydride and amorphous carbon produced by carbonate reduction. This reaction mechanism is similar to the one proposed by the same research group during mechanochemical reduction of CO_2 gas using light metal hydrides [17].

On the basis of previous knowledge, the replacement of gaseous CO_2 and H_2 by solid alkaline carbonates and hydrides to carry out the CO_2 conversion process, presents some advantages. From the point of view of materials manipulation, inorganic carbonates are inexpensive, abundant, and easy to handle under air atmosphere. As an extra advantage, some carbonates are the main product obtained after CO_2 capture by absorbents like Li_4SiO_4 or Na_2ZrO_3 [19–23], then their use as CO_2 source could allow the recycling of degraded absorbents after long operation periods. Also, the use of CO_2 and H_2 storage materials eases transportation and storage. Finally, the reduction of inorganic carbonates reinforces the aim of reusing CO_2 as a feedstock in other chemical processes [24–26]. However, despite the recent advances reported in the current literature, the light carbonates-hydrides mixtures have been poorly explored.

In this work, Li_2CO_3 and MgH_2 were chosen, for the first time to the best of our knowledge, as CO_2 and H_2 portable storage materials to evaluate the direct methanation reaction promoted by

Please cite this article in press as: M.L. Grasso, L.F. Albanesi, S. Garroni et al. Methane production by mechanochemical processing of MgH_2-Li_2CO_3 as sources of H_2 and CO_2 at room temperature. J. CO_2 Util. (2020), https://doi.org/10.1016/j.jcou.2020.101209

high-energy mechanochemical activation. Specifically, the selection of Li_2CO_3 gives the possibility to reuse final products obtained from deteriorated CO_2 absorbents. In addition, the formation kinetics of both CH_4 and H_2 was investigated using theoretical models to fit the time-dependent experimental conversion data. In order to clarify the reaction mechanism of the MgH_2-Li_2CO_3 reaction system, a combination of different techniques for structural, microstructural and chemical characterization of the solids was used and complemented by thermodynamic calculations.

2. Experimental

2.1. Materials preparation

Commercial MgH_2 (Rockwood Lithium, 99.8 %) and Li_2CO_3 (Alfa Aesar, 99 %) powders were used as precursor reagents. Mixtures with different molar ratio of MgH_2:Li_2CO_3, 4:1 and 2:1 were prepared by ball milling (BM). For each mixture, a total amount of 1 g was used, corresponding to 0.59 g MgH_2-0.41 g Li_2CO_3 and 0.42 g MgH_2-0.58 g Li_2CO_3 for 4:1 and 2:1 M ratio, respectively. The procedure for the mechanical treatment consisted in sealing each reagent mixture in a vial and ball milling by using a Spex mixer/mill model 8000 adapted for milling at different rotation speeds. The vial and the ball used are made of stainless steel. The ball milling conditions were: ball mass to powder mass ratio of 1–4, room temperature, an argon pressure of 0.98 atm and rotation speed of 750, 875, 925 and 1000 rpm. The milling was stopped each 5 min, avoiding temperature increase in the milling system.

Because of the air sensitivity of the powders, sample handling was performed under a high-purity argon atmosphere inside a glove box device (MBraun) with oxygen and water levels below 1 ppm.

2.2. Characterization techniques

The structural and morphological properties of the materials were analyzed by X-Ray Powder Diffraction (XRPD) using a Rigaku DMax diffractometer with CuKα radiation tube, Scanning Electron Microscopy (SEM, ZEISS Crossbeam 340 microscope and SEM, FEI Inspect S50) with Energy-Dispersive X-ray Spectroscopy (EDXS) and solid state FTIR (Perkin Elmer Spectrum Series 400). To prevent the sample oxidation during XRPD measurements, an airtight sample holder with Kapton dome was used. A wide peak at lower angle was observed due to kapton contribution. Using the Scherrer equation [27], the crystallite size of the phases before and after milling was calculated using the following peaks: MgH_2 (2θ: 27.9°), $Mg(OH)_2$ (2θ: 18.6°), Li_2CO_3 (2θ: 21.3°), MgO (2θ: 42.9°) and Mg (2θ: 36.6°). Considering that the area of the main peak of each phase is proportional to the amount of that phase in the crystalline sample, estimations of the proportion of X phase respect to the rest of phases all containing Mg were performed. The proportion (P, percent) of MgH_2, Mg, or MgO in the starting material and after mechanochemical milling were calculated from XRPD measurements, using the following equation:

$$P_X = \frac{I_X}{I_{MgH2} + I_{MgO} + I_{Mg}} \cdot 100 \quad (6)$$

where X is the specie of interest and I is the integrated intensity of the most intense reflections of MgH_2 (2θ: 27.9°), MgO (2θ: 42.9°) and Mg (2θ: 36.6°).

For the morphological observations and elemental mapping, powder samples were dispersed on a carbon based tape and coated with gold to improve electrical conductivity. In the case of solid-state FTIR spectroscopy measurements, the powders were mixed with dry KBr and pressed to pellets under air conditions. The presence of carbon-based solids on the final products was investigated by Raman spectroscopy with a confocal microscope (LabRAM HR Evolution Raman microscope) at room temperature using the laser wavelength of 514 nm.

The gaseous phase was followed by gas-chromatography (GC). Hydrogen (H_2), methane (CH_4) and other hydrocarbons were detected using both a Perkin Elmer 8500 and a Fisons 8000 apparatus equipped with a flame ionization (FID) and thermal conductivity (TCD) detectors, respectively. Suitable gas standard mixtures were used to quantify the hydrocarbons production during milling at different times. The conversion values (α) for the gas products CH_4 and H_2 were calculated as follows:

$$\alpha_{CH4} = \frac{n_{CH4}}{n_{CO2}} \quad (7)$$

$$\alpha_{H2} = \frac{n_{H2}}{n_{MgH2}} \quad (8)$$

where nCH_4=moles of CH_4 produced, nCO_2=moles of CO_2 supplied from Li_2CO_3, nH_2= moles of H_2 produced and $nMgH_2$=moles of MgH_2 supplied.

2.3. Thermodynamic calculations

The equilibrium compositions for MgH_2-Li_2CO_3 system as a function of the pressure were calculated using HSC Chemistry Windows, 6.1 version [28]. When all species in a reaction system are given (reactants and products), the software determines the distribution of the products where the Gibbs free energy of the system reaches its minimum at constant temperature. For calculations, H_2:CO_2 molar ratio of: $4MgH_2$:Li_2CO_3; $2MgH_2$:Li_2CO_3; $3.64MgH_2$:Li_2CO_3:0.36 Mg and $1.82MgH_2$:Li_2CO_3:0.18 Mg were taken into account as initial reagents; it was supposed room temperature condition. For these reaction system, the following phases were considered: Ar, CO_2, H_2, CO, O_2, CH_4, C_2H_4, C_2H_6 and H_2O in the gas phase, and Li_2O, LiOH, Li_2CO_3, Li_2C_2, MgH_2, Mg, MgO, $Mg(OH)_2$, $MgCO_3$ and carbon as possible solid products.

3. Results

3.1. Ball milling of MgH_2-Li_2CO_3 system: structural and microstructural analyses

XRPD patterns of the MgH_2-Li_2CO_3 system after milling for different times show the structural and microstructural evolution of the solid phases (Fig. 1). For all cases, a broadening of the peaks was observed due to a gradual modification of microstructural features induced by the mechanical processing. For comparison, the structural study of the reagents before milling shows the high crystallinity of MgH_2, with minor amounts of Mg, and Li_2CO_3 (Fig. S1A). Independently on the milling time and the rotation speed, a remnant of the reactants MgH_2 and Li_2CO_3 as crystalline phases as well as free Mg was identified during mechanochemical processing (Fig. 1A). At higher rotation speeds such as 925 rpm, it is possible to recognize the most intense diffraction peaks of MgO at 42.92° and 62.31°. Progressive formation of MgO was confirmed with the increment of the milling time at 1000 rpm (Fig. 1B); simultaneously Li_2CO_3 and MgH_2 were detected, indicating their incomplete transformation. Other Li-containing phases were not detected with this technique.

The solids obtained after milling of MgH_2-Li_2CO_3 for 720 min using 750 and 1000 rpm were analyzed by FTIR and Raman (Fig. 2). The FTIR results confirm the presence of Li_2CO_3 phase in both samples (Fig. 2A), in agreement with XRPD technique. The bands at

Please cite this article in press as: M.L. Grasso, L.F. Albanesi, S. Garroni et al. Methane production by mechanochemical processing of MgH_2-Li_2CO_3 as sources of H_2 and CO_2 at room temperature. J. CO_2 Util. (2020), https://doi.org/10.1016/j.jcou.2020.101209

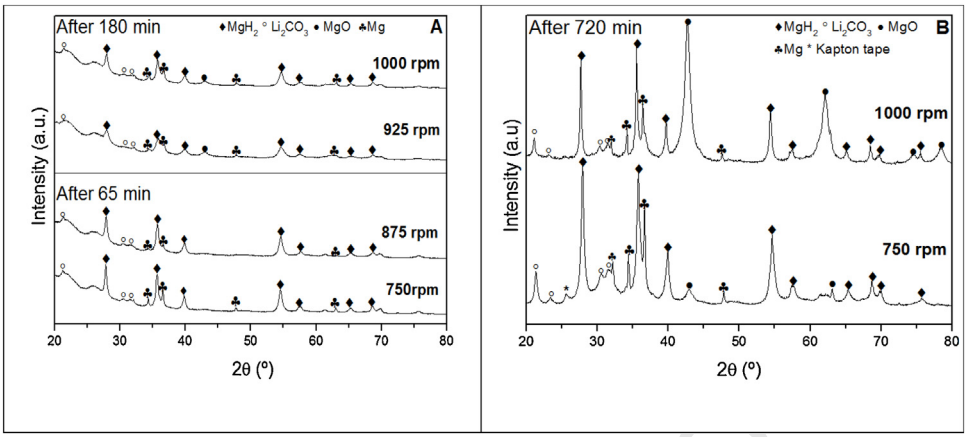

Fig. 1. XRPD patterns after milling of the $4MgH_2$-Li_2CO_3 system at different milling times (A) and rotation speeds (B).

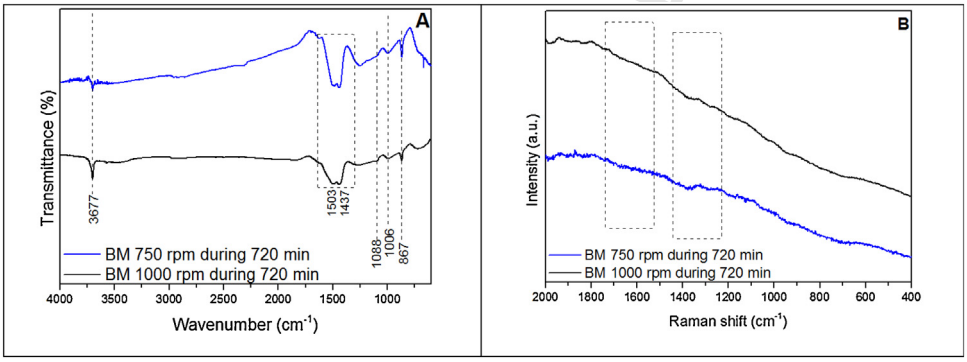

Fig. 2. Solid-state FTIR (A) and Raman spectra (B) of $4MgH_2$-Li_2CO_3 after milling at 750 rpm and 1000 rpm during 720 min.

867, 1503 and 1437 cm^{-1} due to the bending and asymmetric stretching vibrations of Li_2CO_3 were observed simultaneously with a small band at 1088 cm^{-1} due to the stretching vibration [29]. The band identified at 3677 cm^{-1} is related with OH- onto Li^+ and it is ascribed to partial hydroxylation of the sample. Its presence can be interpreted as a result of the reaction between Li_2O with moisture from the air, in agreement with previous work [30]. No evidence of MgO hydroxylation was observed, as it can be inferred by the absence of the stretching vibration at 3699 cm^{-1} [31]. This result is in accordance with the minor $\Delta G°$ value obtained for hydrolysis of Li_2O (-88.1 kJ/mol [28]) respect to MgO (-35.7 kJ/mol [28]) at room temperature, suggesting that Li_2O reacts easily with H_2O from a thermodynamic point of view.

This constitutes an evidence that mechanochemical processing of the MgH_2-Li_2CO_3 mixture for long milling times induces the formation of Li_2O. In addition, Raman measurements were performed to clarify if amorphous carbon was formed as an intermediate of the reaction, as it was observed in similar systems [18]. The Raman spectra shows the absence of both G and D peaks in the region near 1600 and 1350 cm^{-1}, which are ascribed to graphite and defects in carbonaceous solid respectively (Fig. 2B) [32].

The crystallite sizes of the reagents and products were calculated before and after milling using the Scherrer equation (Fig. 3). The values evidence a trend to decrease in grain size with the time and milling rotation speed for the reagents and associated phases (Mg). On the contrary, the phase MgO shows an increment in the grain size during milling probably due to its partial crystallization during mechanical processing.

The morphological characterization of starting powders reveals a uniform distribution of MgH_2 agglomerates with an average size of 180 μm, while for Li_2CO_3 powders display a broad distribution size between 60 and 700 μm (Figs. S1B and S1C, respectively). In both cases, their agglomerates have faceted edges; in particular, partial agglomerate disaggregation was observed for Li_2CO_3. Mechanical milling of the MgH_2-Li_2CO_3 mixture introduces relevant morphological modifications in the starting materials. The size distribution of the agglomerates goes from 40 to 60 microns. The as-milled MgH_2-Li_2CO_3 powders at 750 rpm for 65 and 720 min show agglomerates with sponge-type shape (Figs. 4A and B, respectively). The surface of each agglomerate was analyzed by EDXS element mapping evidencing uniform distribution of magnesium, oxygen and carbon due to a well mixing grade of the initial reagents. In particular, after 65 min of milling, there are smooth particles (red circles) with a chemical composition corresponding to Mg. Long times of milling (720 min) favor the uniform distribution of all elements to sizes lower than 1 μm.

3.2. Gas evolution during milling: Kinetic analysis of the CH_4 and H_2 production

The release of the gaseous species inside the milling chamber was followed by gas chromatography analysis (Fig. 5), taking samples at different reaction times. From short milling times and independently of the energetic conditions, the main products formed by milling of the MgH_2-Li_2CO_3 system were methane (Fig. 5A) and hydrogen (Fig. 5B). Signals corresponding to other hydrocarbons such as ethylene and acetylene were found after

Please cite this article in press as: M.L. Grasso, L.F. Albanesi, S. Garroni et al. Methane production by mechanochemical processing of MgH_2-Li_2CO_3 as sources of H_2 and CO_2 at room temperature. J. CO_2 Util. (2020), https://doi.org/10.1016/j.jcou.2020.101209

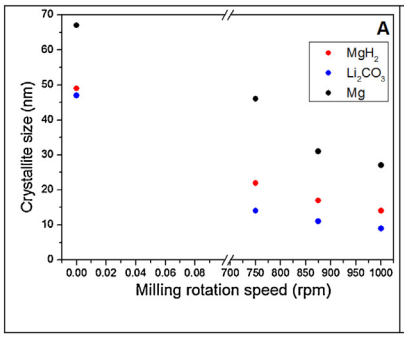

B

Milling rotation speed (65min)	Crystallite size (nm)				
	MgH_2	Li_2CO_3	Mg	MgO	$Mg(OH)_2$
0 rpm	49	47	67	-----	185
750 rpm	23	14	46	-----	-----
875 rpm	17	11	31	7	-----
1000 rpm	14	9	27	9	-----

Fig. 3. Change in the crystallite size as a function of milling rate after 65 min of milling. Plot for the starting reagents (A) and table of all the crystalline species observed (B).

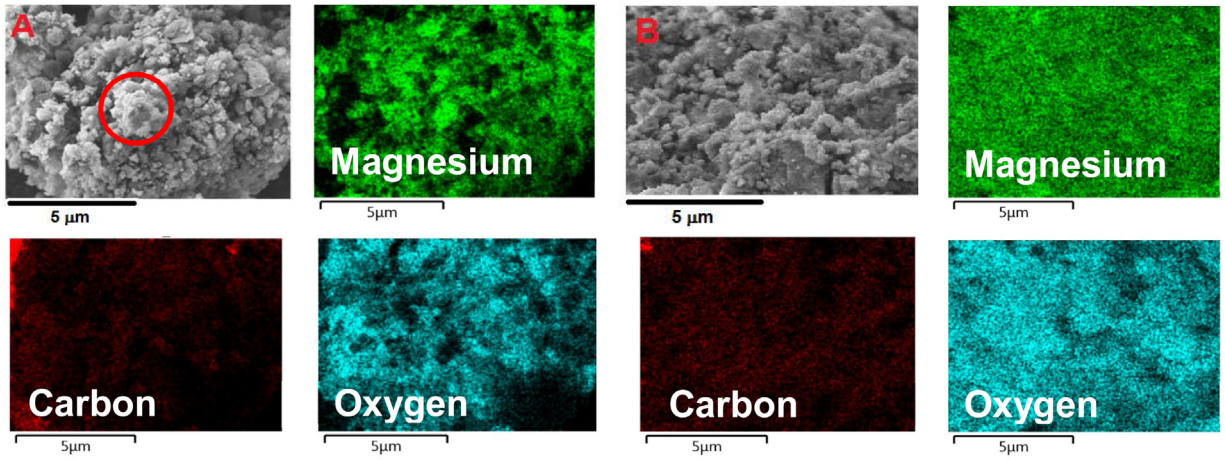

Fig. 4. SEM photographs and elemental mapping after milling of the $4MgH_2$-Li_2CO_3 system at 750 rpm during 65 min (A) and 720 min (B).

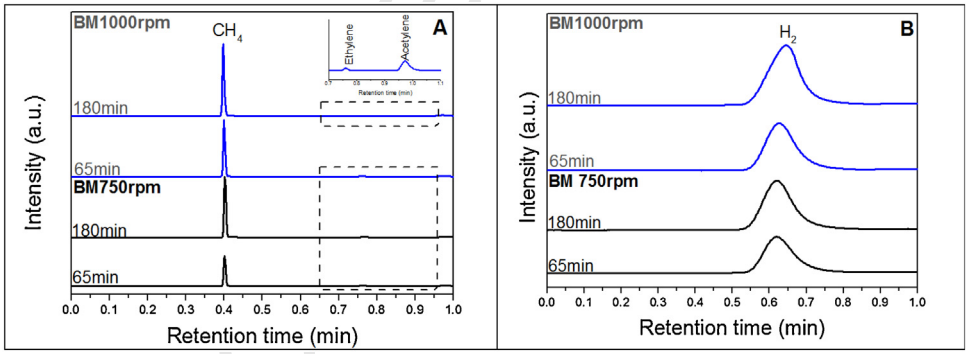

Fig. 5. Chromatograms of the gas products collected during milling of $4MgH_2$-Li_2CO_3 system at 750 rpm and 1000 rpm for different times.

milling at 1000 rpm promoted by high-energy milling conditions. The ethylene and acetylene concentrations were below 1 % for all milling rotation speeds. The presence of CO_2 or CO in the gas phase was not detected in any experimental condition.

Evolution of the moles of CH_4 and H_2 as function of milling time at different speeds (Figs. 6A and B) shows that the amounts of CH_4 and H_2 increase with both parameters. The curves of CH_4 show a quadratic dependence with the milling time increase, while H_2 moles grow following an approximately linear behavior from the beginning of the mechanical processing. In both cases, the moles of H_2 formed at a fix milling time and milling rotation speed are at least two times the moles of CH_4 detected.

To study the influence of H_2:CO_2 molar ratio in the reactivity of the MgH_2-Li_2CO_3 system, the most energetic conditions (1000 rpm) were selected to compare the amount of gas produced with the milling time increase (Fig. S2 and Table S1). The shapes of the curves for methane and hydrogen in the plot look similar. In fact, the amount of H_2 (available in the gas phase) increased due to the rise in the H_2:CO_2 molar ratio and did not have a clear impact on the moles of the CH_4 formed. This result suggests that the mechanism controlling the global process is the same independently of the starting H_2:CO_2 mol ratio.

To analyze the possible mechanism that controls the reaction between MgH_2 and Li_2CO_3 during mechanochemical processing,

Please cite this article in press as: M.L. Grasso, L.F. Albanesi, S. Garroni et al. Methane production by mechanochemical processing of MgH_2-Li_2CO_3 as sources of H_2 and CO_2 at room temperature. J. CO_2 Util. (2020), https://doi.org/10.1016/j.jcou.2020.101209

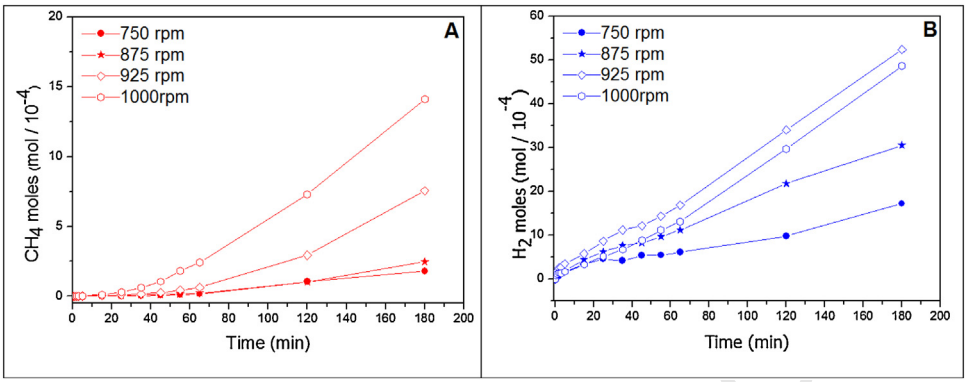

Fig. 6. Moles of CH_4 (A) and H_2 (B) produced during milling of the $4MgH_2$-Li_2CO_3 system for different milling rotation speeds and milling times.

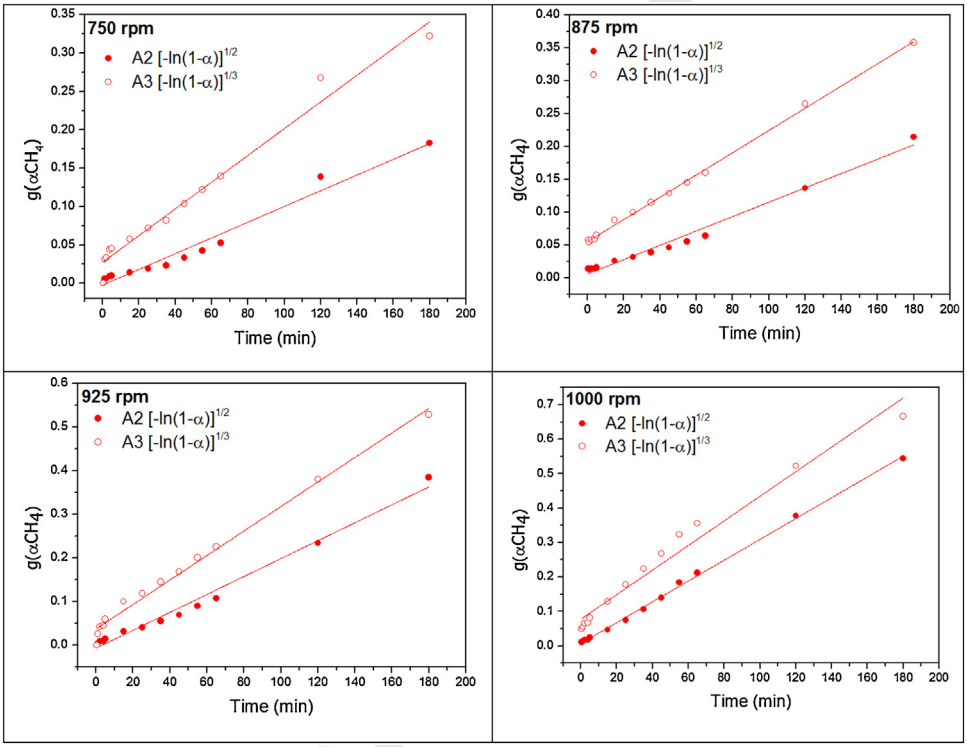

Fig. 7. Fitting of the experimental data for methane conversion using Avrami-Erofeyev models.

the conversion of CH_4 and H_2 was calculated using equations (8), (9) and data from Fig. 6 (Fig S3). These experimental data were fitted using theoretical models (Figs. 7 and 8), i.e. g(α) linearized functions developed for solid state reaction such as Avrami-Erofeyev, Power law and diffusion models (Table 1). These models assume that the solid-state reaction occurs in a single step; however, in many cases, intermediate phases are experimentally observed, indicating a complex reaction mechanism.

In this analysis, the value R^2 (squared correlation coefficient) was chosen as a goodness of fit parameter. R^2 parameter was obtained by fitting the whole range of milling time (up to 180 min). The average value of R^2 parameter for each model proposed by Flanagan et al. [33] is shown in Fig. S4. From this figure it is possible to notice that the rate controlling mechanism for methane and hydrogen production is different. The conversion values (α) for methane adjust well with nucleation models such as Avrami-Erofeyev and Power law (Fig. 7), with R^2 between 0.97 and 0.998. However, Power law is simply a numerical model without a specific association with the physical mechanism. In contrast, the Avrami-Erofeyev exponent describes the feasibility of nucleation and usually provides information about the rate-limiting step and the dimensionality of the growth process.

On the other hand, the geometrical contraction models (R2 and R3) are the most accurate to describe the hydrogen gas formation, with $R^2 = 0.995$ (Fig. 8). These models assume that nucleation occurs rapidly on the surface of the particle, and all particles are equivalent in shape and size. The reaction is usually controlled by the resulting reaction interface progressing toward the center of the particles.

The values of the kinetic rate constant as a function of milling rotation speed obtained from Figs. 7 and 8 are displayed in Table 2. The trend shows that the kinetic rate constant for each model increases with milling rotation speed, showing an enhancement of the conditions for CH_4 and H_2 gas production.

Please cite this article in press as: M.L. Grasso, L.F. Albanesi, S. Garroni et al. Methane production by mechanochemical processing of MgH_2-Li_2CO_3 as sources of H_2 and CO_2 at room temperature. J. CO_2 Util. (2020), https://doi.org/10.1016/j.jcou.2020.101209

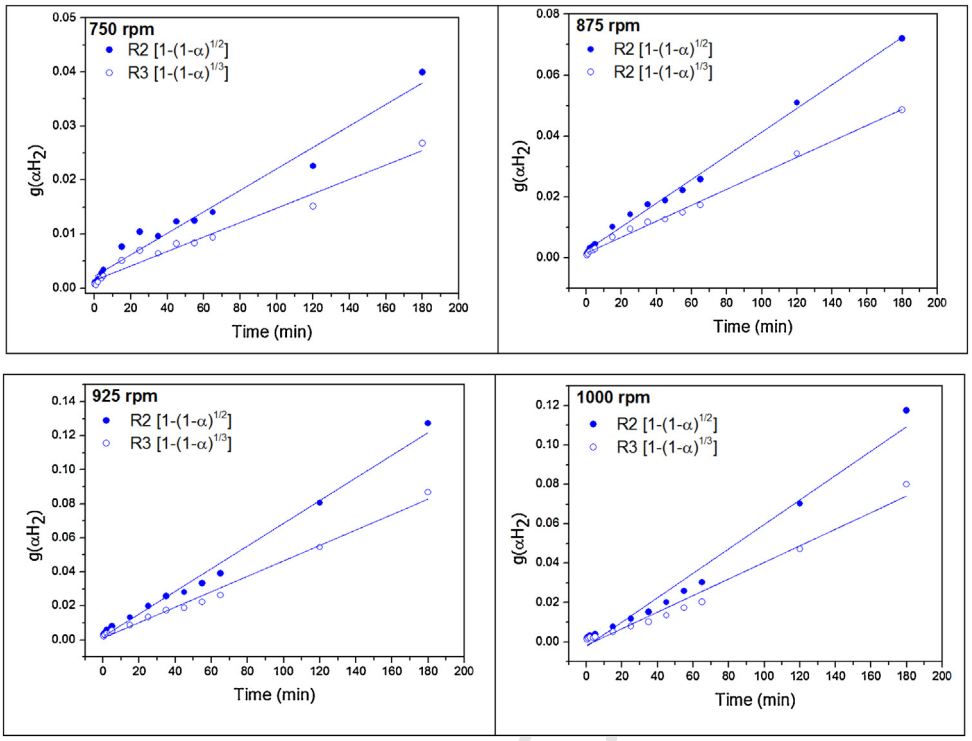

Fig. 8. Fitting of the experimental data for hydrogen conversion using geometrical contraction models.

Table 1
Kinetic models and rate equations used for fitting the conversion of CH_4 and H_2 experimental data. α=conversion (eqs. 8 and 9), k = kinetic rate constant, t = time(s).

Model	Integral form g(α)=kt
Nucleation models	
Power law (P2)	$\alpha^{1/2}$
Power law (P3)	$\alpha^{1/3}$
Power law (P4)	$\alpha^{1/4}$
Avrami-Erofeyev (A2)	$[-\ln(1-\alpha)]^{1/2}$
Avrami-Erofeyev (A3)	$[-\ln(1-\alpha)]^{1/3}$
Geometrical contraction models	
Contracting area (R2)	$[1-(1-\alpha)^{1/2}]$
Contracting volume (R3)	$[1-(1-\alpha)^{1/3}]$
Diffusion models	
1D diffusion (D1)	α^2
2D diffusion (D2)	$[(1-\alpha)\ln(1-\alpha)]+\alpha$
3D diffusion-Jander equation (D3)	$[1-(1-\alpha)^{1/3}]^2$
Reaction zero-order	
Zero-order (F0)	α
First-order (F1)	$-\ln(1-\alpha)$
Second-order (F2)	$(1-\alpha)^{-1}-1$
Third-order (F3)	$0.5[(1-\alpha)^{-2}-1]$

4. Discussion

The reaction between MgH_2 and Li_2CO_3 occurs at room temperature promoted by high-energy milling. Its progress is demonstrated by the gradual formation of both the MgO in the solid phase (Fig. 1) and the mixture CH_4-H_2 in the gas phase (Fig. 4). As an unexpected result, long milling times (720 min) and high energetic conditions (1000 rpm) are not enough to completely consume the reagents. In fact, both MgH_2 and Li_2CO_3 starting materials were identified as crystalline phases after reaction under the most energetic conditions (Fig. 1B). Moreover, after a prolonged milling of 720 min, MgH_2, Mg and MgO are the preponderant phases containing Mg detected by XRPD (Fig. 1); while the presence of LiOH detected by FTIR is an indication of the Li_2O formation during extended high-energetic milling conditions (Fig. 2B).

The thermodynamic calculations for the MgH_2-Li_2CO_3 system at different H_2–CO_2 mol ratio (2:1 and 4:1) were performed to determine the equilibrium composition (Figs. 9A and B). These Figures show the equilibrium composition of the gaseous and solid state species as a function of gas pressure at room temperature. Similar results were obtained in both approaches. It can be noted

Table 2
Reaction rate constants obtained for the CH_4 and H_2 formation using Avrami-Erofeyev model and geometrical contraction model, respectively.

Milling rotation speed	Reaction rate constant (s^{-1}), k for CH_4 data	Reaction rate constant (s^{-1}), k for H_2 data
750 rpm	$1.66.10^{-5}$ (A2)	$3.3.10^{-6}$ (R2)
	$3.33.10^{-5}$ (A3)	$2.21.10^{-6}$ (R3)
875 rpm	$1.66.10^{-5}$ (A2)	$4.8.10^{-6}$ (R2)
	$3.33.10^{-5}$ (A3)	$4.37.10^{-6}$ (R3)
925 rpm	$3.33.10^{-5}$ (A2)	$1.11.10^{-5}$ (R2)
	5.10^{-5} (A3)	$7.55.10^{-5}$ (R3)
1000 rpm	5.10^{-5} (A2)	$1.0.10^{-5}$ (R2)
	$6.67.10^{-5}$ (A3)	$7.03.10^{-5}$ (R3)

Please cite this article in press as: M.L. Grasso, L.F. Albanesi, S. Garroni et al. Methane production by mechanochemical processing of MgH_2-Li_2CO_3 as sources of H_2 and CO_2 at room temperature. J. CO_2 Util. (2020), https://doi.org/10.1016/j.jcou.2020.101209

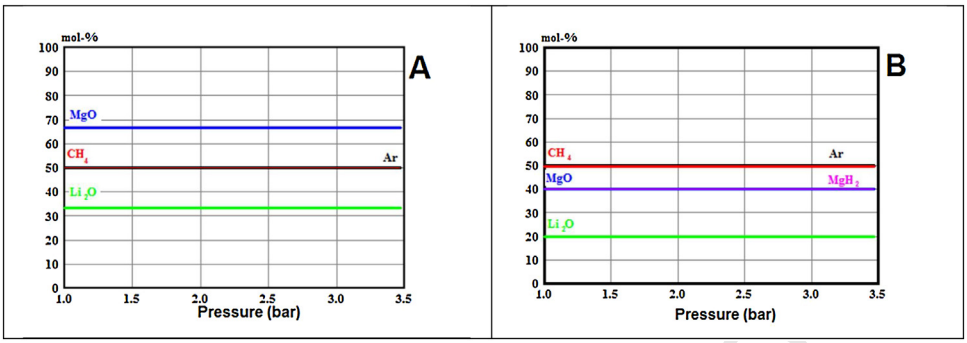

Fig. 9. Equilibrium composition (mol %) as a function of pressure of $2MgH_2$-Li_2CO_3 (A) and $4MgH_2$-Li_2CO_3 (B).

that MgO and Li_2O are stable in the condensed phase in the entire range of pressure investigated, while CH_4 appears as the only product in gas phase (Fig. 9). The equilibrium composition of these phases was constant and independent of the total gas pressure of the system at room temperature. As it was seen for MgH_2-Li_2CO_3 with 2:1 ratio, whole oxidation of MgH_2 to MgO is predicted (Fig. 9A), while for 4:1 ratio, free MgH_2 remains without reacting (Fig. 9B). The global reaction based on these thermodynamic calculations can be expressed for the 2:1 ratio as:

$$2MgH_2(s) + Li_2CO_3(s) \rightarrow 2MgO(s) + Li_2O(s) + CH_4(g) \quad (9)$$

In the case of the 4:1 ratio, it is expected the presence of 2 mol of unreacted MgH_2 in the solid products. For thermodynamic calculations performed considering that the starting MgH_2-Li_2CO_3 mixture contains a molar ratio minor than 2:1 or 4:1 due to partial decomposition of MgH_2 to Mg in the starting mixture (Figs. S5A and S5B, respectively), the formation of C or Li_2C_2 was predicted. From Raman measurements no evidence of the appearance of C (bands at about 1580 and 1340 cm^{-1}) and/or Li_2C_2 (band at 1873 cm^{-1}, [34]) was obtained.

The formation of H_2 in the gas phase was not predicted from thermodynamic calculations independently of the starting MgH_2:Li_2CO_3 molar ratio (Figs. 9 and S5). Its detection during milling of the MgH_2-Li_2CO_3 mixture (Fig. 5) could be related with some kinetic restrictions operating in the reaction system, which hinder its consumption to form CH_4. In fact, the amount of H_2 available in gas phase exceeds the necessary quantity to produce an extra amount of CH_4 (Fig. 6), suggesting that its availability is not a limiting factor. Milling of pure MgH_2, using the same experimental mechanochemical conditions applied to the $2MgH_2$-Li_2CO_3 mixture, demonstrates that H_2 is formed by direct MgH_2 decomposition (Fig. S6):

$$MgH_2(s) \rightarrow Mg(s) + H_2(g) \quad (10)$$

In contrast, no evidence of CO or CO_2 formation was observed after milling pure Li_2CO_3. Moreover, when MgH_2 was milled simultaneously with Li_2CO_3 in the same experimental conditions, H_2 release is promoted (Fig. S6) from the beginning of the reaction. Among the possible reasons, one is that the presence of a second phase with different mechanical properties (Li_2CO_3) modifies the milling conditions, affecting the energy transfer during fracturing and cold working phenomena of the powders. Other possible explanation is that the presence of Li_2CO_3 modifies the stability of MgH_2 by superficial oxidation and favors its decomposition.

Reaction (10) explains the presence of H_2 measured by GC but not envisaged from thermodynamic calculations. As it was previously shown, the amount of H_2 formed exceeds at least in a factor of 2 that corresponding to CH_4 (Fig. 6). According to kinetic studies (Fig. 8), the hydrogen release is controlled by the reaction interface between MgH_2/Mg or MgH_2/MgO. The formation of Mg *via* reaction (10) allows its reaction with Li_2CO_3 to produce CH_4 in a H_2 rich environment:

$$2Mg(s) + 2H_2(g) + Li_2CO_3(s) \rightarrow 2MgO(s) + Li_2O(s) + CH_4(g) \quad (11)$$

Reaction (11) is thermodynamically favored at room temperature [34]. The combination of reactions (10) and (11) gives the global reaction (9), predicted from thermodynamic calculations. Considering that rate constant for the contracting volume is proportional to the rate constant of the interface-controlled reaction and inversely proportional to the particle length [35], the increment in the rate constant with the milling rotation rate (Table 2) can be attributed to the improvement of the microstructure refinement of the Mg based phases (Figs. 3 and 4).

Considering that reaction (10) is a fast process and that it does not control the global reaction rate, reactions (9) and (11) could occur simultaneously to produce CH_4. An inspection of the relative change of the MgH_2 and Mg amounts with the milling time for 750 rpm and 1000 rpm (Table S2) shows that the amount of MgH_2 decreases, while the Mg amount increases. This behavior demonstrates that reaction (10) is actually occurring, justifying the detection of H_2 in the gas phase and the increment in the relative amount of Mg with the milling time. In addition, the amount of MgH_2 decreases due to its consumption by direct reaction (9) or combination of reactions (10) and (11). The formation of CH_4 seems to be kinetically restricted by the high stability observed for Li_2CO_3 under mechanochemical processing. In fact, experimental results demonstrate the absence of CO and CO_2 in the gaseous phase as a carbon source. Moreover, no alternative carbon source in the solid phase, such as amorphous carbon or Li_2C_2, were detected (Figs. 1 and 2). Then, kinetic constrains for CH_4 production involve the formation of Li_2O and MgO through reaction (9) and/or (11). The transfer of oxygen atoms from Li_2CO_3 toward two different oxides is necessary and can possibly be the rate-controlling process. In this context, the nucleation and growth models are suitable to describe the reaction mechanism (Fig. 7).

Finally, in this study it was demonstrated for the first time that Li_2CO_3 and MgH_2 can be used as CO_2 and H_2 sources to effectively produce a CH_4/H_2 fuel mixture at room temperature (see Fig. 10). All resulting products of the mechanochemical treatment of Li_2CO_3 and MgH_2 are used: the CH_4-H_2 mixture as fuels in internal combustion engines /gas turbines; and the Mg-Li oxides as absorbers of CO_2 for the treatment of exhaust gases of a power plant. In the whole cycle process, only MgH_2 is consummated. The new addition of MgH_2 allows starting the cycle again by the reaction with Li carbonate (or Mg carbonate).

Please cite this article in press as: M.L. Grasso, L.F. Albanesi, S. Garroni et al. Methane production by mechanochemical processing of MgH_2-Li_2CO_3 as sources of H_2 and CO_2 at room temperature. J. CO_2 Util. (2020), https://doi.org/10.1016/j.jcou.2020.101209

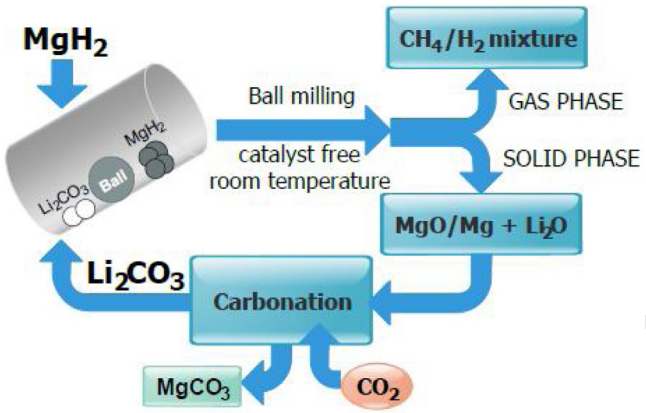

Fig. 10. Schematic representation of the mechanochemical reaction between Li_2CO_3 and MgH_2 and their integration.

By comparison of our mechanochemical processing of MgH_2-Li_2CO_3 with alternative processes to produce CH_4, different advantages emerge. Traditional CO_2 hydrogenation is a process with significant kinetic constrains due to the high stability of CO_2 molecule. Therefore, it requires the utilization of active and selective catalysts to favor this reaction and produce mainly CH_4, avoiding the formation of CO as intermediate product. Even though, CO_2 hydrogenation involves high temperatures, atmospheric pressure and a $4H_2$:$1CO_2$ molar ratio [36,37]. Another process involves MgH_2 to reduce CO_2 without the use of catalysts, but requires 48 h at 450 °C [38]. Although mechanochemical reaction between MgH_2 and CO_2 gas occurs at room temperature, long milling times (24 h) are required to obtain yields lower (6 % and 15 % at 450 rpm and 550 rpm, respectively) [16] than those obtained in this work (3 h of milling, yield of 25 % at 1000 rpm, Table S1). Reaction of magnesite ($MgCO_3$) as CO_2 source with H_2 needs 475–505 °C for the CH_4 production, with simultaneous formation of CO [26].

Recently, the use of dual function materials for CO_2 capture and catalytic conversion to CH_4 allows the temperature to be reduced to about 200 °C, but the use of noble metals is required [39]. Taking advantage of the mechanochemical processing as a simple, efficient and scalable technology, in this work the CO_2 contained in Li_2CO_3 was reduced using MgH_2 to produce CH_4/H_2 fuels at room temperature with high selectivity, avoiding the use of catalyst and/or solvents, minimizing the generation of waste.

5. Conclusions

In this work, the production of the CH_4/H_2 fuel mixtures by high-energy mechanochemical activation of the Li_2CO_3-MgH_2 system at room temperature was studied for the first time. The products were obtained through a free-catalyst reaction, with high selectivity and using Li_2CO_3 and MgH_2 as solid portable sources of CO_2 and H_2, respectively. The analyses done by X-ray diffraction, FTIR and Raman spectroscopies, electron scanning microscopy and gas chromatography techniques to study the evolution of the Li_2CO_3-MgH_2 system during milling was complemented with thermodynamic calculations. Theoretical calculations predict the complete CO_2 reduction to CH_4, with simultaneous formation of MgO and Li_2O. Experimental evidence supports the progressive formation of MgO, MgH_2 consumption and the appearance of Li_2O when milling time increases. The presence of H_2 in the gas phase was due to the high Li_2CO_3 stability and the consequent kinetic restrictions in the CH_4 formation. The conversion of MgH_2-Li_2CO_3 to CH_4/H_2 mixtures depends on the milling time, rotation speed and H_2/CO_2 molar ratio.

The experimental data of CH_4 and H_2 conversion were fitted using theoretical kinetic models with R^2 as a goodness of fit parameter. The best kinetic model for describing the CH_4 evolution was found to the JMA (Johnson-Mehl-Avrami) model. It can be associated with MgO and Li_2O nucleation and their three-dimensional growth along the interface between Li_2CO_3 and Mg/MgH_2. In the case of H_2 release, the contracting volume model fits very well the experimental data and the process is controlled by the reaction interface between MgH_2/Mg or MgH_2/MgO.

Therefore, the combination of carbonates and metal hydrides are promising portable systems for the *in situ* preparation of CH_4/H_2 mixture fuels. The use of Li_2CO_3 as a CO_2 source allows for recycling exhausted absorbents from the post-combustion technologies and to reuse CO_2 efficiently producing in situ fuels with high added value. Currently we are developing alternative methods and innovative explorations to improve the rate of the aforementioned reactions, keeping selectivity and the mild experimental conditions.

CRediT authorship contribution statement

María L. Grasso: Data curation, Validation, Visualization, Formal analysis, Investigation, Writing - original draft. **Luisa Fernández Albanesi:** Data curation, Validation, Investigation, Writing - review & editing. **Sebastiano Garroni:** Conceptualization, Methodology, Investigation, Writing - review & editing, Supervision. **Gabriele Mulas:** Conceptualization, Methodology, Investigation, Writing - review & editing, Supervision. **Fabiana C. Gennari:** Conceptualization, Methodology, Investigation, Writing - original draft, Writing - review & editing, Supervision.

Declaration of Competing Interest

The authors declare that they have no known competing financial interests or personal relationships that could have appeared to influence the work reported in this paper.

Acknowledgements

The present work is part of the CO2MPRISE, "CO_2 absorbing Materials Project- RISE", a project that has received funding from the European Union's Horizon 2020 research and innovation programme, under the Marie Skłodowska-Curie Grant Agreement No 73487[illegible]e work was also supported by CONICET (Consejo Nacional [illegible]nvestigaciones Científicas y Técnicas), ANPCyT–(Agencia Nacional de Promoción Científica y Tecnológica), CNEA

(Comisión Nacional de Energía Atómica) and UNISS (Università degli Studi di Sassari). The authors also thank Bernardo Pentke (Departamento Fisicoquímica de Materiales /CAB- CNEA) for the SEM micrographs and Sebastián Anguiano for the Raman measurements (Laboratorio de Fotónica y Fotoelectrónica /CAB-CNEA).

Appendix A. Supplementary data

Supplementary material related to this article can be found, in the online version, at doi:https://doi.org/10.1016/j.jcou.2020.101209.

References

[1] NASA Global Climate Chage, (2020) . https://climate.nasa.gov/vital-signs/carbon-dioxide/ (Accessed 07 April 2020).
[2] R.K. Pachauri, L. Meyer (Eds.), Climate Change 2014: Synthesis Report, IPCC, Geneva, Switzerland, 2014, pp. 151.
[3] A. Rafiee, K.R. Khalilpour, D. Milani, M. Panahi, Trends in CO_2 conversion and utilization: a review from process systems perspective, J. Environ. Chem. Eng. 6 (2018) 5771–5794, doi:http://dx.doi.org/10.1016/j.jece.2018.08.065.
[4] H. Sun, Y. Zhang, Z. Guan, J. Huang, C. Wu, Direct and highly selective conversion of captured CO_2 into methane through integrated carbon capture and utilization over dual functional materials, J. CO2 Util. 38 (2020) 262–272, doi:http://dx.doi.org/10.1016/j.jcou.2020.02.001.
[5] NIST Chemistry WebBook, (2018) . https://webbook.nist.gov/chemistry/ (Accessed 30 March 2020).
[6] S. Specchia, S. Tacchino, V. Specchia, Facing the catalytic combustion of CH_4/H_2 mixtures into monoliths, Chem. Eng. J. 167 (2-3) (2011) 622–633, doi:http://dx.doi.org/10.1016/j.cej.2010.10.051.
[7] Y. Yu, W. Lin, L. Li, Z. Zhang, Effects of hydrogen addition on the combustion characteristics of diesel fuel jets under ultra-high injection pressures, Int. J. Hydrogen Energy 45 (17) (2020) 10592–10601, doi:http://dx.doi.org/10.1016/j.ijhydene.2019.08.242.
[8] N. Muradov, Chapter 8. transition to low- and zero- carbon energy and fuels, Liberating Energy From Carbon: Introduction to Decarbonization, first ed., Springer, New York, 2014, pp. 279–323.
[9] M.L. Grasso, J. Puszkiel, L. Fernández Albanesi, M. Dornheim, C. Pistidda, F.C. Gennari, CO_2 utilization for methan production via catalytic promoted by hydrides, Phys. Chem. Chem.Phys. 21 (2019) 19825–19843, doi:http://dx.doi.org/10.1039/C9CP03826D.
[10] M.L. Grasso, J. Puszkiel, C. Pistidda, A. Santoru, M. Dornheim, F.C. Gennari, CO_2 reactivity with Mg2NiH4 synthesized by in situ monitoring mechanical milling, Phys. Chem. Chem.Phys. 22 (2020) 1944–1952, doi:http://dx.doi.org/10.1039/C9CP05697A.
[11] C. Bolm, J.G. Hernández, Mechanochemistry of gaseous reactants, Angew. Chem. Int. Ed. Engl. 58 (11) (2019) 3285–3299, doi:http://dx.doi.org/10.1002/anie.201810902.
[12] P. Baláž, M. Achimovičová, M. Baláž, P. Billik, Z. Cherkezova-Zheleva, J.M. Criado, F. Delogu, E. Dutková, E. Gaffet, F.J. Gotor, R. Kumar, I. Mitov, T. Rojac, M. Senna, A. Streletskii, K. Wieczorek-Ciurowa, Hallmarks of mechanochemistry: from nanoparticles to technology, Chem. Soc. Rev. 42 (2013) 7571–7637, doi:http://dx.doi.org/10.1039/C3CS35468G.
[13] G. Mulas, R. Campesi, S. Garroni, F. Delogu, C. Milanese, Hydrogenation of Carbon monoxide over nanostructured systems: mechanochemical approach, Appl. Surf. Sci. 257 (2011) 8165–8570, doi:http://dx.doi.org/10.1016/j.apsusc.2011.03.024.
[14] V. Farina, N.S. Gamba, F. Gennari, S. Garroni Sebastiano, F. Torre, A. Taras, S. Enzo, G. Mulas, CO_2 hydrogenation induced by mechanochemical activation of olivine with water under CO_2 atmosphere, Front. Energy Res. 7 (2019) 107–117, doi:http://dx.doi.org/10.3389/fenrg.2019.00107.
[15] F. Torre, V. Farina, A. Taras, C. Pistidda, A. Santoru, J. Bednarcik, G. Mulas, S. Enzo, S. Garroni, Room temperature hydrocarbon generation in olivine powders: effect of mechanical processing under CO_2 atmosphere, Powder Technol. 364 (2020) 915–923, doi:http://dx.doi.org/10.1016/j.powtec.2019.10.080.
[16] B.-X. Dong, L.-Z. J.Zhao, Y.-L. Wang, W.-L. Teng, L. Liu, ME Wang, Chanochemical synthesis of COx-free hydrogen and methane fuel mixtures at room temperature from light metal hydrides and carbon dioxide, Appl. Energy 204 (2017) 741–748, doi:http://dx.doi.org/10.1016/j.apenergy.2017.07.088.
[17] K. Pu, Y. Yang, X.Q, M. Gao, Y. Liu, H. Pan, Room temperature conversion of Carbon Dioxide into fuels gases by mechanochemically reacting with metal hydrides, Chem. Select. 2 (2017) 5244–5247, doi:http://dx.doi.org/10.1002/slct.201700834.
[18] B.-X. Dong, L. Wang, J. Zhao, Y.-L. Teng, C. Ping, W. Zhu, H.-B. Chen, W.-L. Liu, Highly selective room-temperature catalyst- free reduction of alkaline carbonates to methane by metal hydrides, Energy Technol. 7 (2019) 1800719, doi:http://dx.doi.org/10.1002/ente.201800719.
[19] M.L. Grasso, M.V. Blanco, F. Cova, J.A. González, P. Arneodo Larochette, F.C. Gennari, Evaluation of the formation and carbon dioxide capture of Li_4SiO_4 using in situ synchrotron powder X-ray diffraction studies, Phys. Chem. Chem. Phys. 20 (2018) 26570–26579, doi:http://dx.doi.org/10.1039/c8cp03611.
[20] X. Yan, Y. Li, X. Ma, J. Zhao, Z. Wang, Perfomance of Li_4SiO_4 material for CO_2 capture: a review, Int. J. Mol. Sci. 20 (2019) 928–950, doi:http://dx.doi.org/10.3390/ijms20040928.
[21] Y. Zhang, Y. Gao, H. Pfeiffer, B. Louis, L. Sun, D. OHare, Q. Wang, Recent advances in lithium containing ceramics based sorbents for high-temperature CO_2 capture, J. Mater. Chem. A Mater. Energy Sustain. 7 (2019) 7962–8005, doi:http://dx.doi.org/10.1039/C8TA08932A.
[22] D. Peltzer, J. Múnera, L. Cornaglia, Operando Raman spectroscopic studies of lithium zirconates during CO2 capture at high temperature, RSC Adv. 6 (2016) 8222–8231, doi:http://dx.doi.org/10.1039/C5RA21970A.
[23] I. Alcérreca-Corte, E. Fregoso-Israel, H. Pfeiffer, CO_2 absorption on Na_2ZrO_3: a kinetic analysis of the chemisorption and diffusion processes, J. Phys Chem. C 112 (2008) 6520–6525, doi:http://dx.doi.org/10.1021/jp710475g.
[24] D. Jagadeesan, M. Eswaramoorthy, C.N.R. Rao, Investigations of the conversion of inorganic carbonates to methane, Chem. Sus. Chem. 2 (2009) 878–882, doi:http://dx.doi.org/10.1002/cssc.200900152.
[25] S. Lux, G. Baldauf-Sommerbauer, M. Siebenhofer, Hydrogenation of inorganic metal carbonates: a review on its potential for carbon dioxide utilization and emission reduction, Chem. Sus. Chem. 11 (2018) 3357–3375, doi:http://dx.doi.org/10.1002/cssc.201801356.
[26] G. Baldauf-Sommerbauer, S. Lux, W. Aniser, M. Siebenhofer, Reductive calcination of mineral magnesite: hydrogenation of carbon dioxide without catalysts, Chem. Eng. Technol. 39 (11) (2016) 2035–2041, doi:http://dx.doi.org/10.1002/ceat.201600094.
[27] L. Alexander, P.H. Klug, Determination of crystalline size with the X-Ray spectrometer, J. Appl. Phys. 21 (1950) 137–147, doi:http://dx.doi.org/10.1063/1.1699612.
[28] H.S.C. Outokumpu, Chemistry For Windows, Version 6.1, Outokumpu Research Oy, Finland, 2009.
[29] P. Pasierb, S.K. omornicki, M. Rokita, M. Rękas, Structural properties of Li_2CO_3–$BaCO_3$ system derived from IR and Raman spectroscopy, J. Mol. Struct. 596 (1–3) (2001) 151–156, doi:http://dx.doi.org/10.1016/S0022-2860(01)00703-7.
[30] G. Weber, E. Sciora, J. Guichard, F. Bouyer, I. Bezverkhyy, Investigation of hydrolysis of lithium oxide by thermogravimetry, calorimetry and in situ FTIR spectroscopy, J. Therm. Anal. Calorim. 132 (2) (2018) 1055–1064, doi:http://dx.doi.org/10.1007/s10973-017-6943-7.
[31] A. Ansari, A. Ali, M. Asif, Shamsuzzaman, Microwave-assisted MgO NPs catalyzed one-pot multicomponent synthesis of polysubstituted steroidal pyridines, New J. Chem. 42 (2018) 184–197.
[32] J. Hong, M.K. Park, E.J. Lee, D.E. Lee, D.S. Hwang, S. Ryu, Origin of new broad raman d and g peaks in annealed graphene, Sci. Rep. 3 (2012) 2700.
[33] A. Khawam, D. Flanagan, Solid state kinetic models: basics and mathematical fundamentals, J. Phys. Chem. B 110 (2006) 17315–17328, doi:http://dx.doi.org/10.1021/jp062746a.
[34] N. Tian, C. Hua, Z. Wang, L. Chen, Reversible reduction of Li_2CO_3, J. Mater. Chem. A Mater. Energy Sustain. 3 (2015) 14173–14177, doi:http://dx.doi.org/10.1039/C5TA02499D.
[35] Y. Pang, Q. Li, A review on kinetic models and corresponding analysis methods for hydrogen storage materials, Int. J. Hydrogen Energy 41 (2016) 18072–18087, doi:http://dx.doi.org/10.1016/j.ijhydene.2016.08.018.
[36] B.C. Sempuga, Y. Yao, CO_2 hydrogenation from a process synthesis perspective: setting up process targets, J. Co2 Util. 20 (2017) 34–42, doi:http://dx.doi.org/10.1016/j.jcou.2017.05.004.
[37] S. Saeidi, N.A.S. Amin, M.Reza Rahimpour, Hydrogenation of CO_2 to value-added products-A review and potential future developments, J CO_2 Utilization 5 (2014) 66–81, doi:http://dx.doi.org/10.1016/j.jcou.2013.12.005.
[38] J. Zhao, Y.-F. Wei, Y.-L. Cai, L.-Z. Wang, J. Xie, Y.-Lei. Teng, W. Zhu, M. Shen, B.-X. Dong, Highly selective and efficient reduction of CO_2 to methane by activated alkaline earth metal hydrides without a catalyst, ACS Sustain. Chem. Eng. 7 (2019) 4831–4841, doi:http://dx.doi.org/10.1021/acssuschemeng.8b05177.
[39] M.S. Duyar, S. Wang, M.A. Arellano-Treviño, R.J. Farrauto, CO_2 utilization with a novel dual function material (DFM) for capture and catalytic conversion to synthetic natural gas: an update, J. Co_2 Util. 15 (2016) 65–71, doi:http://dx.doi.org/10.1016/j.jcou.2016.05.003.

Please cite this article in press as: M.L. Grasso, L.F. Albanesi, S. Garroni et al. Methane production by mechanochemical processing of MgH_2-Li_2CO_3 as sources of H_2 and CO_2 at room temperature. J. CO_2 Util. (2020), https://doi.org/10.1016/j.jcou.2020.101209